Modeling the effect of line profile variation on optical critical dimension metrology

Thomas A. Germer

Optical Technology Division
National Institute of Standards and Technology,
Gaithersburg, Maryland 20899

ABSTRACT

We investigate the effects that variations in profile have on specular and diffuse reflectance from a grating consisting of parallel lines. We investigate, as an example, a nominal grating consisting of photoresist or silicon lines on a silicon substrate, having a vertical sidewall angle, a width of 100 nm, a pitch of 200 nm, and a height of 200 nm. We model the effects of variations by calculating the reflectance of multiple 25-line superstructures, in which the positions of the line edges are randomly modulated about their nominal profile. We study line-edge variation, line-position variation, and random edge variation in order to test the hypothesis that the reflectance of a grating with variations in line profile can be approximated by the reflectance of a grating with uniform lines having the average line profile. We find that the reflected field can be approximated by the mean field reflected by a distribution of periodic gratings and that the field does not represent the field from the average profile. When fitting results to more than one modeled parameter, the changes that are observed can be enough to shift the deduced parameter in some cases by more than the rms variation of that parameter. We also investigate the diffuse scattering by the grating by considering the diffraction orders of the 25-line period. The intensity distribution and the polarization of the diffuse scattering are found to be different for line-width variation and line-position variation.

Keywords: gratings, line-edge variation, optical critical dimension metrology, scatterometry

1. INTRODUCTION

The reflectance of a periodic array of lines on a surface can be very sensitive to the profile of that structure. The semiconductor industry has capitalized on this sensitivity to measure line widths and profiles of micro-fabricated structures.[1-8] Referred to as non-imaging optical critical dimension metrology (OCD), measurements generally consist of recording the reflectance or polarization as a function of incident angle or wavelength from a periodic test structure. Comparison of the measurement with a library of simulated results for a variety of different possible profiles yields the one which matches the data best. The technique has also been referred to as *scatterometry* in the industry, although rarely does it make use of the diffusely scattered light or anything but the specular reflectance.

While extremely sensitive to details of the profile, OCD instruments have not yielded ideal agreement with other metrology methods.[9] An assumption that is generally made in the interpretation of data is that the structure is indeed periodic, and that any deviation from periodicity gives the same result as some "average" profile. For example, the reflectance data from a grating with variations in line width would be fit to a model that assumes a fixed line width, and the resulting best fit line width would be taken to be the average line width of that grating. In this paper, we investigate the validity of this assumption by performing Monte Carlo (MC) simulations on extended gratings with randomized profiles. We find that deviations from periodicity do not give the same result as the field from the average profile. Rather, the reflected field can be approximated by the mean field reflected by a distribution of periodic profiles. Furthermore, the best fit simple profile to the MC simulated data can be shifted by a large amount from that predicted by the average profile. This study is an extension of another[10] that studied a larger variety of profile variations, including sidewall profile, line height, and trench depth, but which did not include a photoresist grating or perform more than one spectral analysis.

Metrology, Inspection, and Process Control for Microlithography XXI, edited by Chas N. Archie
Proc. of SPIE Vol. 6518, 65180Z, (2007) · 0277-786X/07/$18 · doi: 10.1117/12.704246

Inspection of patterned devices often uses dark field detection of scattered light. Detecting foreign particles or pattern defects requires the signal from the defect to stand out above the background caused by the pattern itself. It is therefore useful to understand the nature of the background signal. Therefore, a second part of this research includes a study of the light diffusely scattered by the random profile.

In Section 2, we outline the theoretical approach used to perform the MC simulations and describe a mean-field model used to approximate the results. In Section 3, we present the results of those simulations. Finally, in Section 4, we draw some conclusions from this work.

2. THEORY

2.1. Grating Simulations

We use the rigorous coupled wave (RCW) analysis for surface relief gratings developed by Moharam, *et al.*,[11,12] with a modification suggested by Lalanne and Morris,[13] Granet and Guizal,[14] and Li[15] to improve the convergence of the calculations for transverse-magnetic (TM) polarization. This method solves the electromagnetic problem for a plane wave incident upon a medium having a dielectric function $\varepsilon(x,y,z)=\varepsilon_j(x)$, which is periodic in x, independent of y, and independent of z within each of a finite number of layers, indicated by index j. The solution requires Fourier series expansions of $\varepsilon_j(x)$ and $1/\varepsilon_j(x)$ for each layer. In practice, the Fourier series is truncated at some maximum order N.

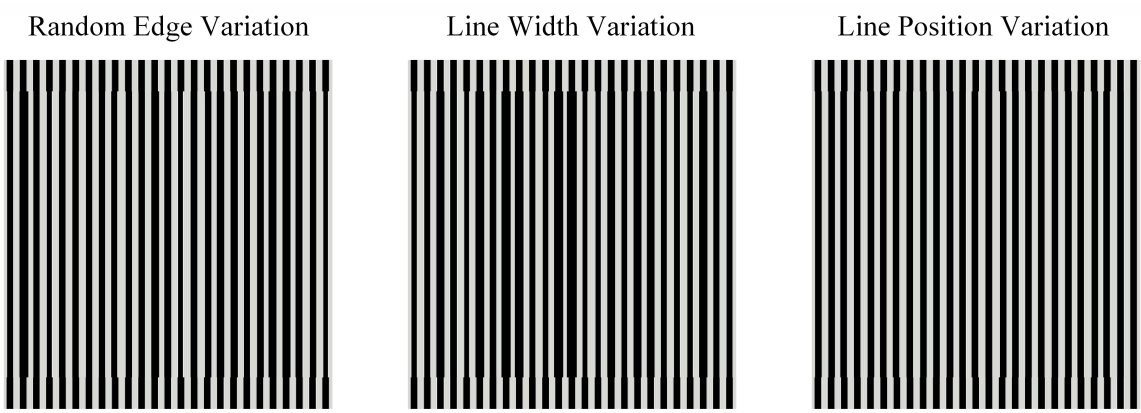

FIGURE 1. Realizations of 25-line gratings with (left) random edge variation, (middle) line width variation, and (right) line position variation. The diagrams show an unperturbed grating on the topand bottom. The lines are shown in black.

2.2. Monte Carlo Simulations

We begin by considering an unperturbed grating having a period Λ_0. To simulate variations in the profile, we create random profiles having a total period $\Lambda_M = M\Lambda_0$ (M an integer) and solve for the scattering amplitude using the RCW method on this larger period. Generally, the unperturbed grating gives rise to diffraction at discrete directions, which when the light is incident perpendicular to the lines is given by

$$\sin\theta_i = \sin\theta + i\lambda/\Lambda_0 , \quad (1)$$

where θ is the incident angle, θ_i is the diffracted angle, and λ is the wavelength of the light. The simulated profiles having the longer period give rise to diffraction at additional directions, such that i takes on fractional values (*i.e.*, iM is an integer). We will denote these fractional orders as *diffuse* orders, since they do not exist for the primary period, and as M increases, the number of these orders expands into a diffuse continuum as would be expected from a non-periodic structure.

In this study, we considered variations in the line edge position. We let Δx_j^L and Δx_j^R be deviations of the left and right edges of the *j*-th line. We create realizations of the random profile, using a pseudo-random number generator having a normal distribution with standard deviation σ. We further consider three different sub-cases of line edge variation. For *line position variation*, we let $\Delta x_j^L = \Delta x_j^R$; for *line width variation*, we let $\Delta x_j^L = -\Delta x_j^R$; and, for *random edge variation*, we let Δx_j^L and Δx_j^R be independent. Figure 1 shows examples of realizations of each of these three cases. In all calculations for the simulation of line edge variation, since the side walls are vertical, only one *z*-level is required in the RCW calculation.

For each case, simulations were performed for 40 realizations of the surface profile. The mean and the standard error for each measurable parameter were found. We used $M = 25$ lines for each realization. The nominal pitch Λ_0 was 200 nm, the height was 200 nm, and the nominal width was 100 nm. The simulations had a Fourier truncation order of $N = 200$. The optical constants of the substrate were those appropriate for silicon. The optical constants for the lines were either those appropriate for silicon or for a photoresist. For spectroscopic reflectance simulations, the wavelength was varied from 250 nm to 600 nm. For the diffuse scattering calculations, the wavelength was fixed at 532 nm.

Simulations were performed for two incident orthogonal polarizations at normal incidence and 70° incidence perpendicular to the lines. The Stokes parameters for incident light linearly polarized at an angle of 45°,

$$\begin{aligned} R_0 &= \tfrac{1}{2}|r_{\mathrm{TE}}|^2 + \tfrac{1}{2}|r_{\mathrm{TM}}|^2 \\ R_1 &= \tfrac{1}{2}|r_{\mathrm{TE}}|^2 - \tfrac{1}{2}|r_{\mathrm{TM}}|^2 \\ R_2 &= \mathrm{Re}(r_{\mathrm{TE}}{}^* r_{\mathrm{TM}}) \\ R_3 &= \mathrm{Im}(r_{\mathrm{TE}}{}^* r_{\mathrm{TM}}) \end{aligned} \tag{2}$$

are presented, where r_{TE} and r_{TM} are the reflectance coefficients for light polarized with the electric field and magnetic fields along the lines, respectively.

2.3. Mean-Field Model

We compared the MC simulation results to those of an approximate model to answer the question of whether or not the field reflected by a random pattern is the average of the field reflected by a distribution of periodic patterns. If the scattering by the lines is dominated by the structure of each individual line, rather than by line-line interactions, then we would expect this condition to be true.

If we consider the field scattered by a periodic array of lines having width *w* to be $\mathbf{E}(w)$, then the field averaged over a normal distribution of the width is given by

$$\langle \mathbf{E} \rangle_w = \frac{1}{\sigma_w \sqrt{2\pi}} \int \mathrm{d}w\, \mathbf{E}(w) \exp[-(w-w_0)^2 / 2\sigma_w{}^2] \tag{3}$$

where w_0 and σ_w are the mean and standard deviation of *w*, respectively. We refer to this model as the *mean-field model*. For variations in line width, since the parameter σ is the rms variation of a single edge, it must be borne in mind that comparisons between the Monte Carlo models must be performed such that $\sigma_w = \sigma\sqrt{2}$ for random edge variation, and $\sigma_w = 2\sigma$ for line width variation. Eq. (3) is evaluated by 4-point Gaussian-Hermite integration. The mean field model is attractive, if it proves to be accurate, because simulations required to evaluate Eq. (3) are performed anyway during construction of a scatterometry library. A similar model can be generated by considering the mean intensity. We do not show results for the mean-intensity model, because they were substantially poorer than those for the mean-field model.

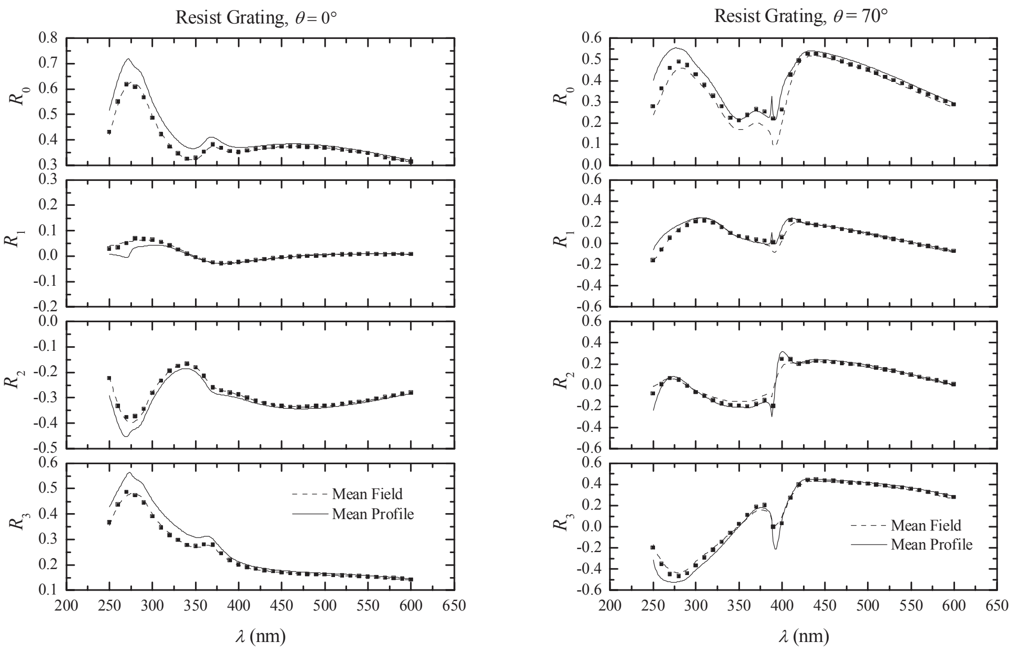

FIGURE 2. Simulated Stokes parameters for zero-order diffraction (specular reflection) from random resist gratings as a function of wavelength: (symbols) the Monte-Carlo simulations for gratings having random edge variation with σ= 10 nm, (solid curves) simulated using the unperturbed profile, and (dashed curves) simulated using the mean field model. The light was incident at (left) 0° and (right) 70°. The incident light was polarized at 45°.

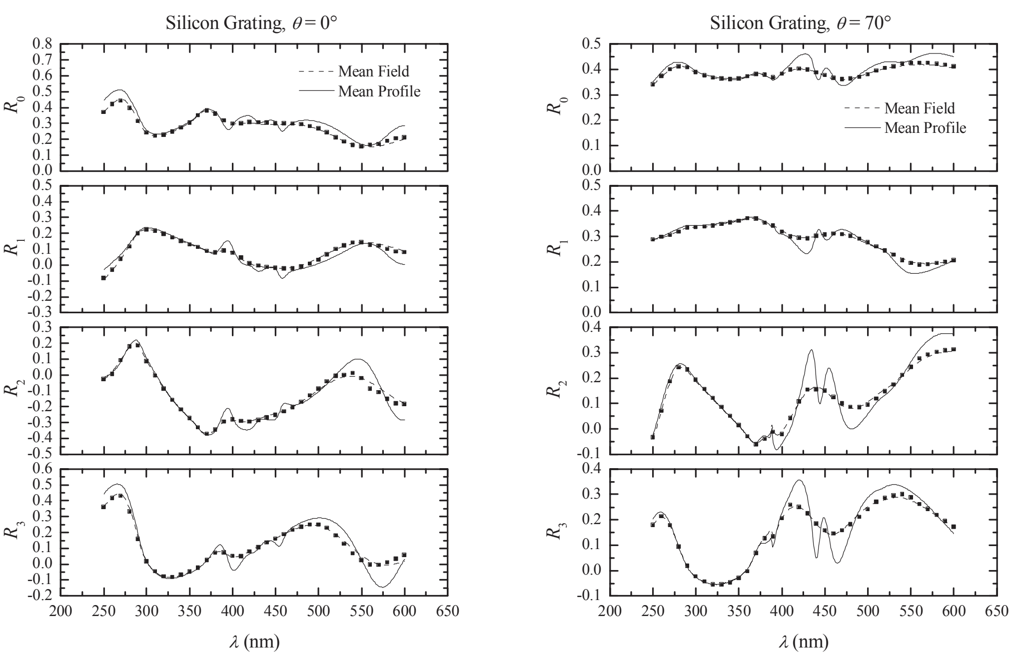

FIGURE 3. Simulated Stokes parameters for zero-order diffraction (specular reflection) from random silicon gratings as a function of wavelength: (symbols) the Monte-Carlo simulations for gratings having random edge variation with σ= 10 nm, (solid curves) simulated using the unperturbed profile, and (dashed curves) simulated using the mean field model. The light was incident at (left) 0° and (right) 70°. The incident light was polarized at 45°.

3. RESULTS AND DISCUSSION

3.1. Specular Reflection

Figures 2 and 3 show the MC-simulated spectral dependence of the Stokes parameters for the zero-order diffraction (specular direction) for random edge variation with $\sigma = 10$ nm for the photoresist silicon gratings, respectively, each at 0° and 70° illumination. This degree of variation was chosen to be very large, about five times that typically acceptable on a production line. Shown with the MC results are the predictions of RCW for the nominal profile and the mean-field model. The results show striking differences between the MC-simulated results for the random grating and the results for the nominal grating. Sharp features associated with the nominal grating are often not observed in the random grating, and even slowly varying features show large shifts. These results clearly demonstrate that modeling a grating with random edge variation with a nominal profile with no edge variation can lead to large discrepancies in the Stokes parameters.

Non-linear least-square fits of the MC-simulated spectra to simple gratings and to the mean-field model were performed using a Levenberg-Marquardt algorithm.[16] Local mean-square minimization works well when good estimates of the fitting parameters are known (in this case, the nominal profile) and allows for greater precision than that which can be obtained by a fixed-grid library search. We chose four different simple gratings and the mean field model to fit to:

1. Binary grating (vertical sidewall), varying only the width.
2. Binary grating (vertical sidewall), varying the width and height.
3. Trapezoidal grating, varying the top and bottom widths.
4. Trapezoidal grating, varying the top and bottom widths and the height.
5. Mean field model, varying line width and variation parameter (σ_w)

We also considered three different data sets for each grating:

1. The Stokes parameters: R_0, R_1, R_2, and R_3.
2. The ellipsometry parameters: $\alpha = R_1/R_0$ and $\beta = R_2/R_0$.
3. The s- and p- reflectances: $R_s = R_0+R_1$ and $R_p = R_0-R_1$

The data within each data set were equally weighted. The results of the fits are not shown in Figs. 2 and 3 because they tended to be very close to their respective nominal curves and the resulting figures would have been too crowded. The best fit model parameters, however, and the root-mean-squares (rms) of the residuals are given in Table 1.

We point out several observations of the results outlined in Table 1. In a number of cases, the deviation of the extracted width from the mean width of the lines is large compared to the variation parameter $\sigma = 10$ nm. For example, when the width and height were varied during a fit to data for s- and p- reflectances for the photoresist grating illuminated at normal incidence, the best fit width deviated from the nominal value by over four times the variation parameter. If we allow the profile sidewall to deviate from vertical, the sidewall angle can show significant deviation from the nominal value. For example, when top and bottom widths and the height were varied during a fit to the Stokes parameters for a photo resist grating illuminated at normal incidence, the best fit sidewall deviated from vertical by nearly 19°. In nearly all cases, the rms residual is very large. The deviations that are observed are consistent with many of the parameters being highly coupled; that is, the rms residual is a long, narrow valley in two or more parameters, and a small change in the curve can shift the location of the minimum by a relatively large amount. The fact that the modeled curves are not particularly good fits to the data (in this case represented by the MC results) makes the valleys flatter and seriously degrades the sensitivity of the results.

In most of the cases, the mean-field model significantly improves the fit, as measured by the rms residual. However, given typical repeatability statistics for measurements (on the order of 0.001 for any of the measurands), the mean-field model rarely yielded an rms residual that would be dominated by the repeatability of the measurement. For most of the data sets, the best fit values for the width and σ_w were close to the nominal values, 100 nm and 14.1 nm (10 nm × $\sqrt{2}$), respectively. However, in the case of each of the photoresist data sets with an incident angle of 70°, both of these values differed by quite a bit. It is not clear what the cause of that discrepancy is, but these fits were at most only marginally better than the fits to the simple profiles.

TABLE 1. Results of least-square fits to the Monte-Carlo results for random edge variation with σ = 10 nm. Each block of results represents a set of different fits to a single set of data, showing the parameters that were adjusted during each fit. The line had a nominal width of 100 nm and a height of 200 nm. The expected value of σ_w is 14.1 nm.

Photoresist grating

	0°					70°				
	top (nm)	bottom (nm)	height (nm)	σ_w (nm)	rms	top (nm)	bottom (nm)	height (nm)	σ_w (nm)	rms
Stokes	102.34	---	---	---	0.0295	103.07	---	---	---	0.0348
	102.45	---	199.66	---	0.0295	107.34	---	193.15	---	0.0262
	85.31	116.80	---	---	0.0252	98.51	109.20	---	---	0.0335
	83.50	117.38	202.04	---	0.0249	101.71	116.02	192.63	---	0.0228
	99.06	---	---	14.05	0.0041	101.83	---	---	8.56	0.0191
α–β	100.01	---	---	---	0.0216	100.82	---	---	---	0.0823
	100.02	---	200.23	---	0.0216	105.96	---	193.46	---	0.0681
	92.47	107.53	---	---	0.0206	103.28	97.15	---	---	0.0811
	84.67	115.15	203.38	---	0.0191	105.78	106.24	193.44	---	0.0681
	99.99	---	---	13.03	0.0079	102.06	---	---	6.48	0.0629
s-p	104.81	---	---	---	0.0410	105.14	---	---	---	0.0399
	143.31	---	181.14	---	0.0312	107.26	---	195.03	---	0.0352
	84.25	118.51	---	---	0.0348	93.02	122.45	---	---	0.0208
	134.90	146.71	183.07	---	0.0314	95.49	122.46	196.94	---	0.0176
	98.02	---	---	13.97	0.0051	103.45	---	---	6.66	0.0251

Silicon grating

	0°					70°				
	top (nm)	bottom (nm)	height (nm)	σ_w (nm)	rms	top (nm)	bottom (nm)	height (nm)	σ_w (nm)	rms
Stokes	98.37	---	---	---	0.0424	100.95	---	---	---	0.0339
	98.95	---	198.46	---	0.0420	101.32	---	199.19	---	0.0338
	94.55	104.48	---	---	0.0392	98.27	104.60	---	---	0.0330
	94.59	104.49	199.95	---	0.0391	98.66	105.11	199.15	---	0.0329
	99.11	---	---	13.26	0.0099	100.42	---	---	13.66	0.0045
α–β	97.84	---	---	---	0.1760	100.22	---	---	---	0.0809
	98.29	---	198.51	---	0.1747	100.26	---	199.81	---	0.0809
	95.18	100.36	---	---	0.1735	99.97	100.47	---	---	0.0809
	95.94	100.30	199.07	---	0.1730	100.03	100.47	199.83	---	0.0809
	98.39	---	---	12.30	0.0481	100.30	---	---	13.72	0.0123
s-p	98.54	---	---	---	0.0474	101.31	---	---	---	0.0285
	98.87	---	197.16	---	0.0465	100.65	---	204.37	---	0.0274
	84.07	108.70	---	---	0.0263	100.62	101.93	---	---	0.0284
	84.35	108.83	199.22	---	0.0262	99.20	101.81	204.64	---	0.0272
	98.65	---	---	12.82	0.0009	100.13	---	---	12.58	0.0037

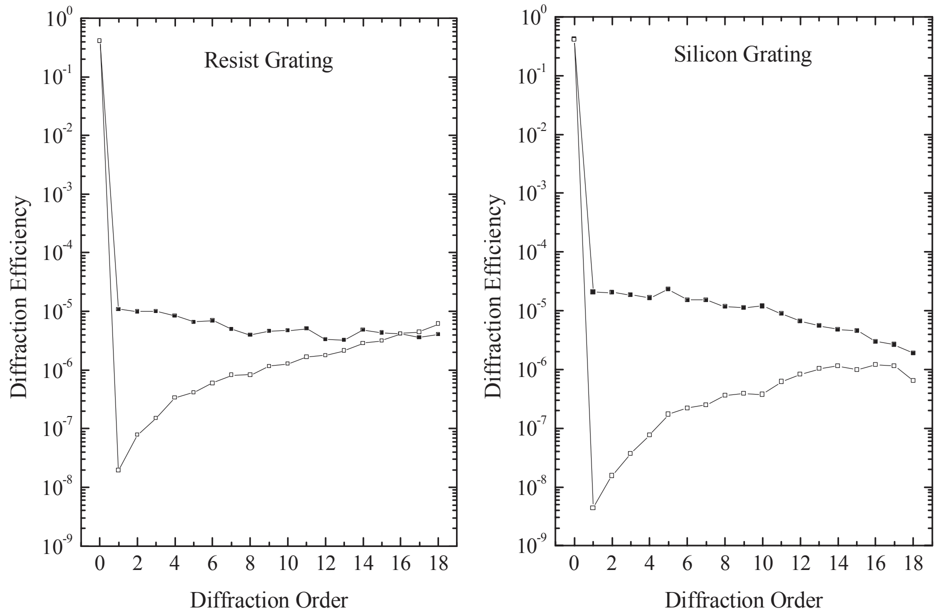

FIGURE 4. Diffraction efficiency as a function of diffraction order calculated for (solid symbols) random width variation and (open symbols) random position variation and for (left) the resist grating and (right) the silicon grating. The variation magnitude is σ = 1 nm, the incident angle is 70°, and the incident light is polarized at 45°.

3.2. Diffuse Reflection

We restrict our results of diffuse scattering to that of line width variation and line position variation having a small amount of variation (σ= 1 nm) and illuminated with 532 nm at 70° incidence. Figure 4 shows the diffraction efficiency of the different orders associated with the 5 μm superstructure period for both the photoresist and silicon gratings. Because the period of the grating, 200 nm, is less than half the wavelength, there are no diffracted orders arising from the fundamental period of the grating. For that reason, there is a large zero-order peak, and because the variation is small, the efficiency of the other orders are all orders of magnitude less intense.

With the exception of the zero-order efficiency, the variation from one diffraction order to another in Fig. 4 is smooth, suggesting that the results are indicative of a random grating of infinite extent. That is, if the period were doubled, the new orders would lie along the same curve, except shifted vertically by a factor of two to keep the total integrated non-specular efficiency constant. One could also estimate the angular distribution of scattered light for an infinite grating from these curves. It is interesting to note the difference between the angular distribution of the light scattered by line-width variation and that scattered by line-position variation. Line-position variation contributes almost no scattered light in the near-specular direction, while scattering by line-width variation has much weaker angle dependence. If we were to introduce inter-line correlations, we would expect to find that the angular dependence of the scatter would be affected.

Previous work on diffuse scatter by smooth surfaces has shown that the polarization of the scattered light can be used to distinguish amongst different scattering sources.[17-21] For example, roughness of each of the two interfaces of a dielectric film scatter with different polarization states, allowing their scatter to be distinguished and the roughness of each interface quantified. In Fig. 5, we show a similar effect for the scatter by a random grating. The normalized Stokes parameters are shown for line-width variation and line-position variation. The results shown in Fig. 5 do not depend upon the amplitude of the variation, provided the variation is small (less than a few nanometers). The two types of variation show a clear and measurable difference in their polarization states. Like the case of roughness of a thin film, one needs to know the details of the unperturbed system in order to analyze the scattered light.

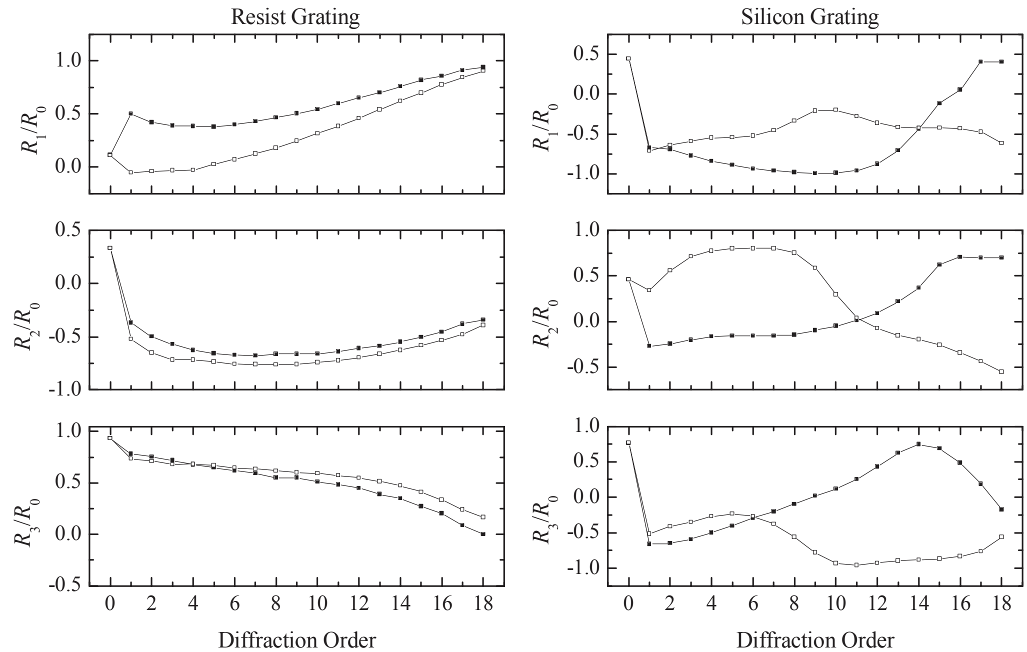

FIGURE 5. The normalized Stokes parameters as a function of diffraction order calculated for (solid symbols) random width variation and (open symbols) random position variation and for (left) the resist grating and (right) the silicon grating. The variation magnitude is $\sigma = 1$ nm, the incident angle is 70°, and the incident light is polarized at 45°.

Furthermore, perturbations which are too large become difficult to analyze because the polarization states are no longer independent. The finding that the scattered light has well-defined polarization states may also help to improve the signal-to-noise ratio during dark-field detection of defects and particles on these gratings.

3.3. Relationship to line-edge and line-width roughness

This study only investigated the effects of line profile shape and did not consider variations in that profile along the *y* direction. The latter variations are commonly referred to as line-edge roughness (LER) and line-width roughness (LWR) when the position and width vary along the line, respectively. LER and LWR are considered important to microfabrication because they may have an effect on device performance and limit the precision of critical-dimension scanning electron microscopy (CD-SEM). The effects of LER and LWR on specular diffraction might be expected to follow those of line position variation and line width variation, respectively, provided the correlation length of the roughness in the *y* direction is significantly larger than the period. It waits to be seen, until full three-dimensional simulations are performed, what the effects are of short correlation length roughness.

4. CONCLUSIONS

This article described some Monte Carlo simulations of reflection and scattering by randomized gratings. The results indicate that non-imaging optical critical dimension measurements do not necessarily yield information about the average profile of the grating. A mean-field model is proposed that yields improved comparisons, but is in itself imperfect and needs refinement. Measurements of diffuse scatter by randomized gratings may yield information about the type of variation (line width versus line position) that exists in a grating.

5. ACKNOWLEDGMENTS

The author would like to thank Drs. Heather Patrick, Krzysztof Michalski, Ravikiran Attota, Robert Larrabee, Egon Marx, and Richard Silver for many useful discussions.

REFERENCES

1. S. A. Coulombe, B. K. Minhas, C. J. Raymond, S. Sohail, H. Naqvi, and J. R. McNeil, "Scatterometry measurement of sub-0.1 µm linewidth gratings," J. Vac. Sci. Technol. B **16**, 80-87 (1998).
2. H.-T. Huang, W. Kong, and F. L. Terry, Jr., "Normal-incidence spectroscopic ellipsometry for critical dimension monitoring," Appl. Phys. Lett. **78**, 3983-3985 (2001).
3. J. R. Marciante, N. O. Farmiga, J. I. Hirsh, M. S. Evans, and H. T. Ta, "Optical measurement of depth and duty cycle for binary diffraction gratings with subwavelength features," Appl. Opt. **42**, 3234-3240 (2003).
4. B. K. Minhas, S. A. Coulombe, S. S. H. Naqvi, and J. R. McNeil, "Ellipsometric scatterometry for the metrology of sub-0.1-µm-linewidth structures," Appl. Opt. **37**, 5112-5115 (1998).
5. X. Niu, N. Jakatdar, J. Bao, and C. J. Spanos, "Specular Spectroscopic Scatterometry," IEEE Trans. Semiconductor Manufacturing **14**, 97-111 (2001).
6. C. J. Raymond, M. R. Murnane, S. S. H. Naqvi, and J. R. McNeil, "Metrology of subwavelength photoresist gratings using optical scatterometry," J. Vac. Sci. Technol. B **13**, 1484-1495 (1995).
7. C. J. Raymond, M. R. Murnane, S. L. Prins, S. Sohail, H. Naqvi, J. R. McNeil, and J. W. Hosch, "Multiparameter grating metrology using optical scatterometry," J. Vac. Sci. Technol. B **15**, 361-368 (1997).
8. W. Yang, J. Hu, R. Lowe-Webb, R. Korlahalli, D. Shivaprasad, H. Sasano, W. Liu, and D. S. L. Mui, "Line-Profile and Critical-Dimension Monitoring Using a Normal Incidence Optical CD Metrology," IEEE Trans. Semiconductor Manufacturing **17**, 564-572 (2004).
9. V. A. Ukraintsev, "A comprehensive test of optical scatterometry readiness for 65 nm technology production," in *Metrology, Inspection, and Process Control for Microlithography XX*, C. N. Archie, ed., Proc. SPIE **6152**, 61521G-1 (2006).
10. T. A. Germer, "Effect of line and trench profile variation on specular and diffuse reflectance from a periodic structure," J. Opt. Soc. Am. A **24**, in press (2007).
11. M. G. Moharam, E. B. Grann, D. A. Pommet, and T. K. Gaylord, "Formulation for stable and efficient implementation of the rigorous coupled-wave analysis of binary gratings," J. Opt. Soc. Am. A **12**, 1068-1076 (1995).
12. M. G. Moharam, D. A. Pommet, E. B. Grann, and T. K. Gaylord, "Stable implementation of the rigorous coupled-wave analysis for surface-relief gratings: enhanced transmittance matrix approach," J. Opt. Soc. Am. A **12**, 1077-1086 (1995).
13. P. Lalanne and G. M. Morris, "Highly improved convergence of the couple-wave method for TM polarization," J. Opt. Soc. Am. A **13**, 779-784 (1996).
14. G. Granet and B. Buizal, "Efficient implementation of the coupled-wave method for metallic lamellar gratings in TM polarization," J. Opt. Soc. Am. A **13**, 1019-1023 (1996).
15. L. Li, "Use of Fourier series in the analysis of discontinuous periodic structures," J. Opt. Soc. Am. A **13**, 1870-1876 (1996).
16. W. H. Press, S. A. Teukolsky, W. T. Vetterling, and B. P. Flannery, *Numerical Recipes in C: The Art of Scientific Computing*, (Cambridge University, 1992).
17. T. A. Germer and C. C. Asmail, "Polarization of light scattered by microrough surfaces and subsurface defects," J. Opt. Soc. Am. A **16**, 1326-1332 (1999).
18. T. A. Germer, "Angular dependence and polarization of out-of-plane optical scattering from particulate contamination, subsurface defects, and surface microroughness," Appl. Opt. **36**, 8798-8805 (1997).
19. T. A. Germer, C. C. Asmail, and B. W. Scheer, "Polarization of out-of-plane scattering from microrough silicon," Opt. Lett. **22**, 1284-1286 (1997).
20. T. A. Germer, "Measurement of roughness of two interfaces of a dielectric film by scattering ellipsometry," Phys. Rev. Lett. **85**, 349-352 (2000).
21. T. A. Germer, "Polarized light scattering by microroughness and small defects in dielectric layers," J. Opt. Soc. Am. A **18**, 1279-1288 (2001).